PNAS
www.pnas.org

Supplementary Information for

A Novel Autophagic Mechanism Mediating Lipid Droplet Catabolism in Hepatocytes

Ryan J. Schulze, Eugene W. Krueger, Shaun G. Weller, Carol A. Casey, Micah B. Schott, and Mark A. McNiven

Paste corresponding author name here
Email: mcniven.mark@mayo.edu

This PDF file includes:

Supplementary text
Figures S1 to S5
Legends for Movies S1 to S4

Other supplementary materials for this manuscript include the following:

Movies S1 to S4

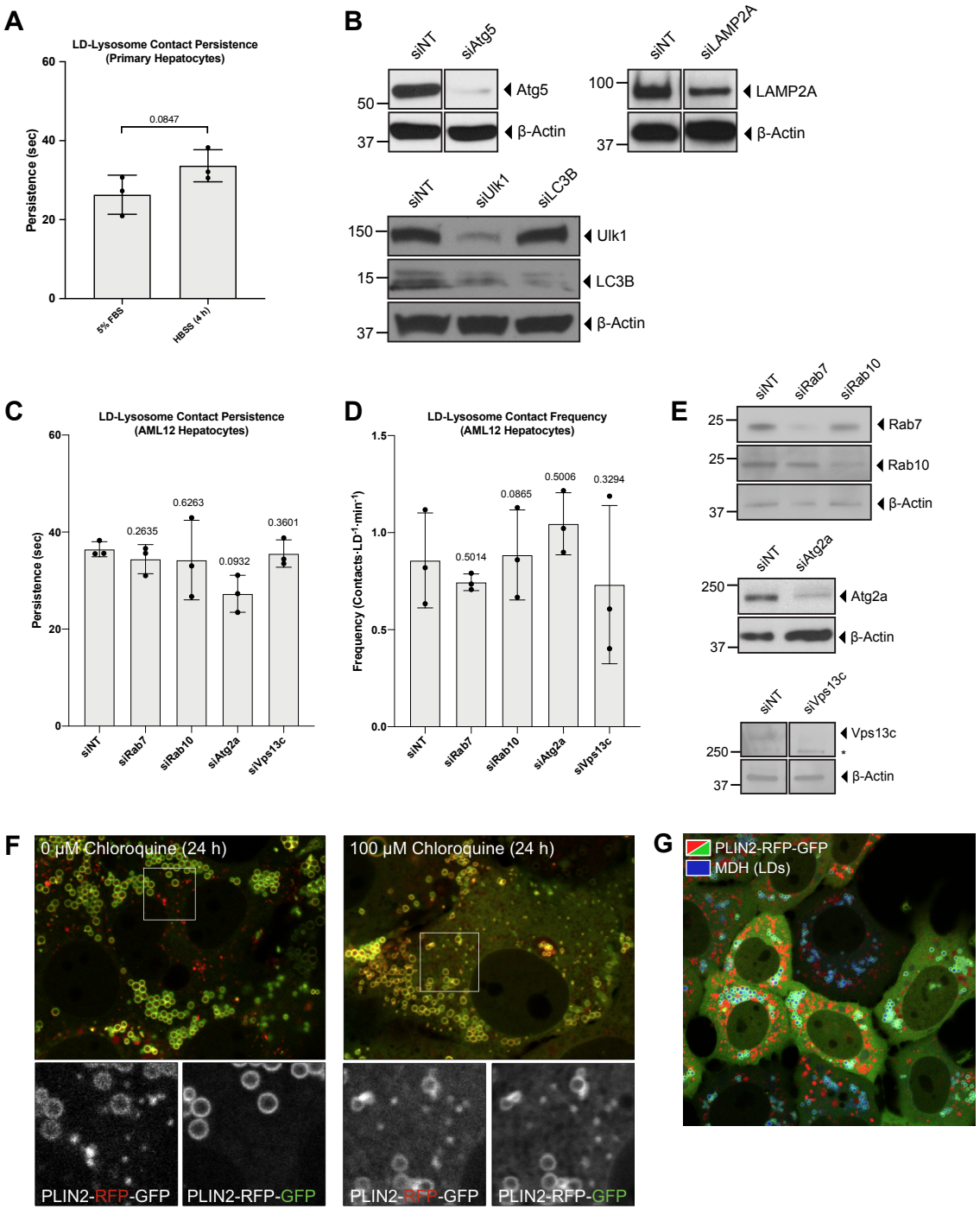

Fig. S1. Frequent interactions between hepatocellular lysosomes and LDs support LD protein transfer. (A) Primary rat hepatocytes were subjected to an overnight lipid load followed by a 4 h period of culture in William's E + 5% FBS or HBSS, to parallel the starvation conditions performed for our electron microscopy experiments in Figs. 2 and 3. Shown is a summary of LD-lysosome contact persistence from n = 3 independent experiments, where at least ten movies were captured for each condition per experiment. p = 0.0847 as measured by paired t-test. Error bars reflect SD. (B) Immunoblotting to demonstrate the knockdown efficiency of siAtg5, siUlk1, siLC3B, and siLAMP2A treatments in the experiments used in Fig. 1C/E. (C-E) Knockdowns of macrolipophagy components (Rab7, Rab10) or lipid transporters (Atg2a, Vps13c) have no

observable effect on LD-lysosome contact persistence (C) or frequency (D). Data represents quantification from three independent experiments in which at least five movies were analyzed per experiment for each condition. Displayed statistics from paired *t*-test. Error bars reflect SD. (E) Immunoblotting to demonstrate the knockdown efficiency of siRab7, siRab10, siAtg2a, or siVps13c treatments. (F) AML12 mouse hepatocytes were transfected with the mRFP1-EGFP-PLIN2 reporter and loaded overnight with 150 μM oleate:BSA. Cells were then treated for an additional 24 h +/- 100 μM chloroquine to neutralize the pH within the lysosomal lumen. As shown at right, treatment with chloroquine results in a retention of EGFP+ signal within lysosome structures, indicating uptake of the reporter into the lysosome. (G) AML12 mouse hepatocytes were stably transfected with the mRFP1-EGFP-PLIN2 reporter and loaded overnight with 150 μM oleate:BSA to stimulate LD production. As shown, there is a significant accumulation of RFP+ puncta throughout the cytoplasm of the cells despite being cultured under basal growth conditions.

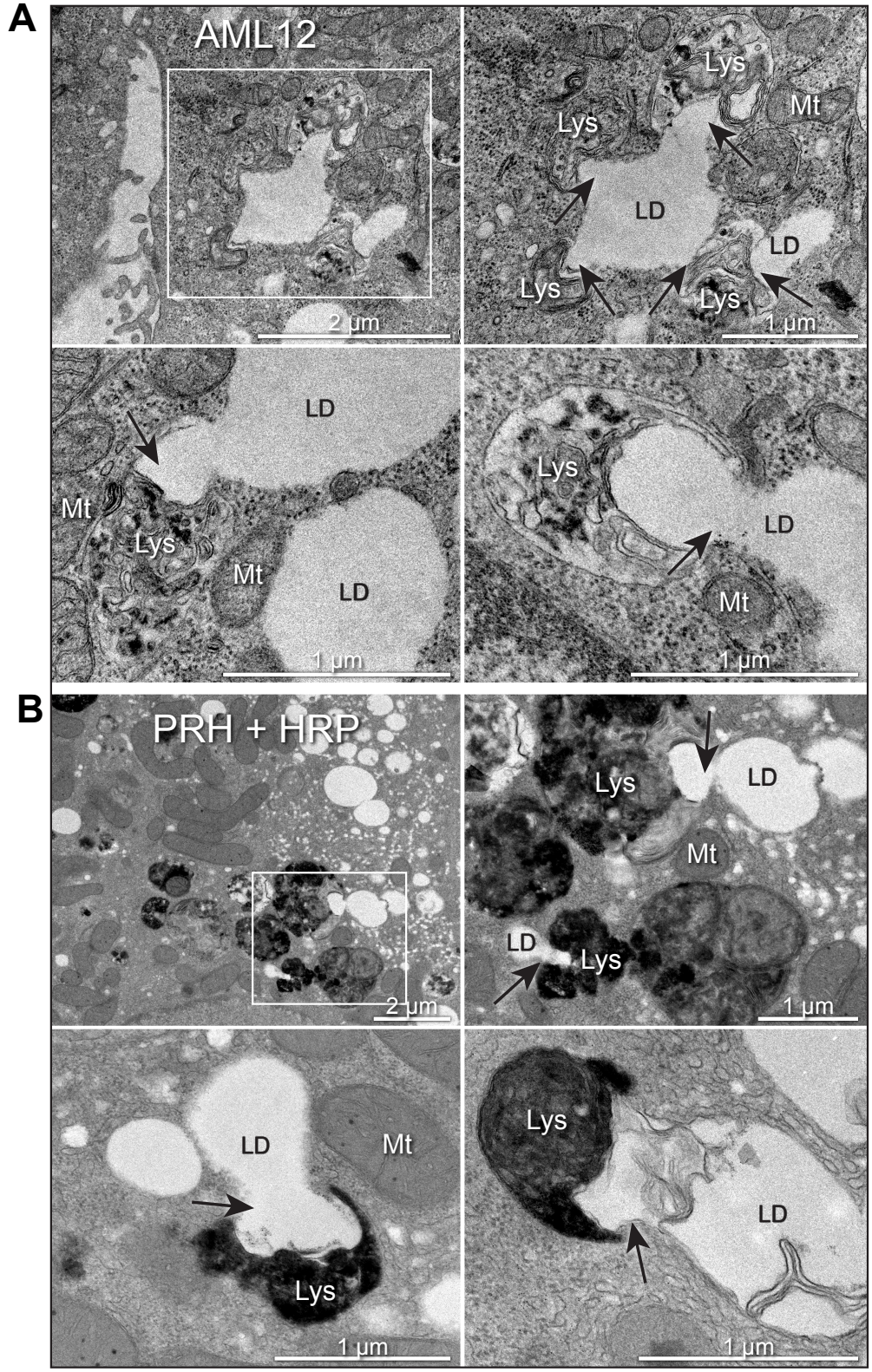

Fig. S2. Additional examples of LD-lysosomal interplay in hepatocytes (A) Electron micrographs of AML12 mouse hepatocytes subjected to culture in media containing 150 µM oleic acid overnight (to stimulate LD formation) then serum-starved in HBSS for 4 h before fixation and

processing for TEM. Note multiple profiles of LDs with clear instances of direct lipid transfer into the lysosomal compartment (arrows). Also, note the presence of mitochondria that are frequently found near these events. (B) Electron micrographs of primary rat hepatocytes pretreated for 60 min with 5 mg/ml horseradish peroxidase, washed 3X, and chased for 150 min at 37°C in label-free medium to enhance the visualization of the terminal endocytic compartment. Note the dark reaction product confirms that acidic lysosomes are the structures interacting with LDs.

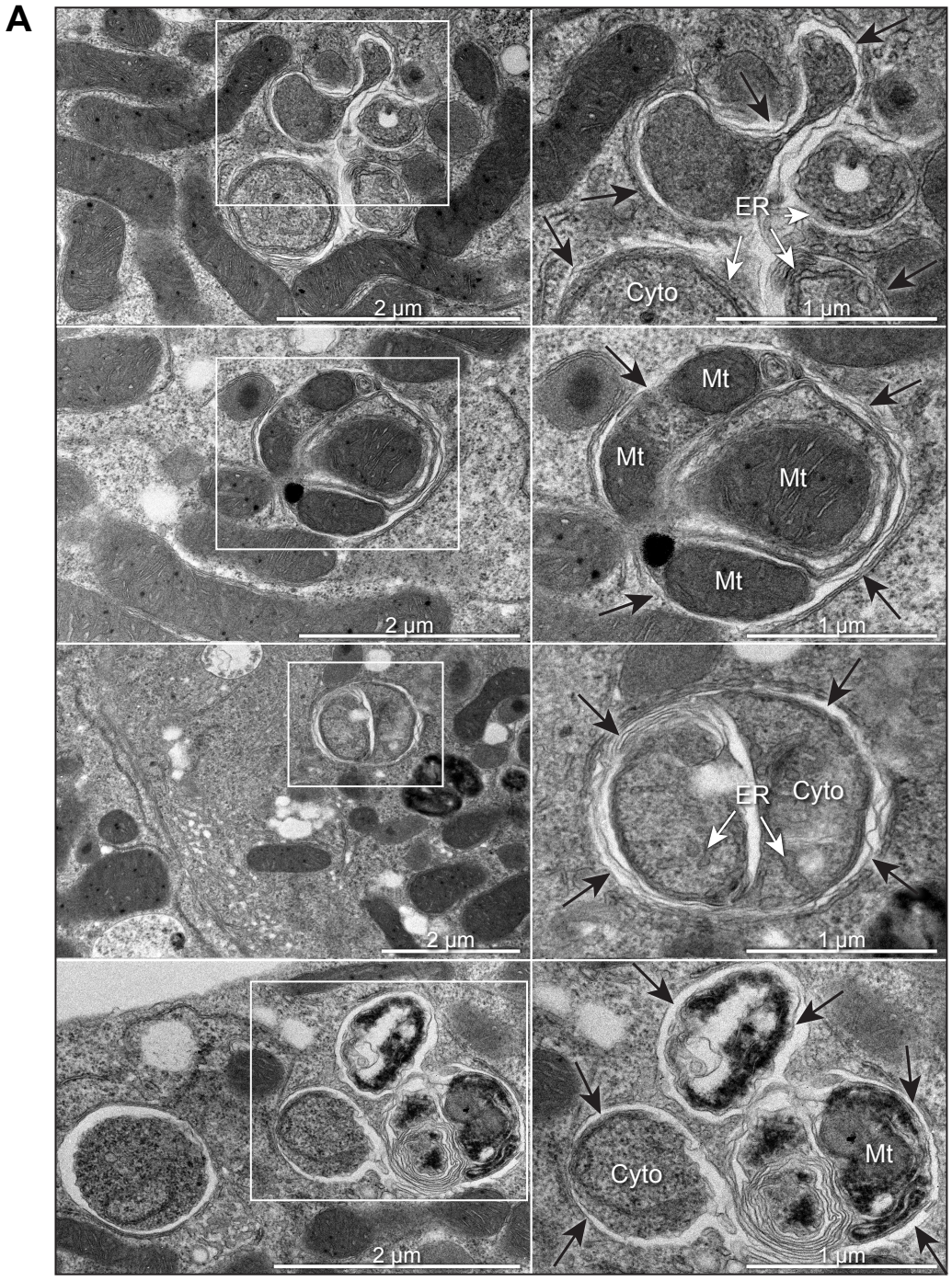

Fig. S3. Examples of canonical macroautophagy in serum-starved hepatocytes. (A) Electron micrographs from primary rat hepatocytes showing the presence of double-membrane structures that we frequently observe in starved cells. These double membranes (arrows) are often observed surrounding cytoplasm, ER, or mitochondria, likely indicating their engulfment within a canonical autophagosome. Note that these double-membrane structures are very rarely observed surrounding LDs in these cells.

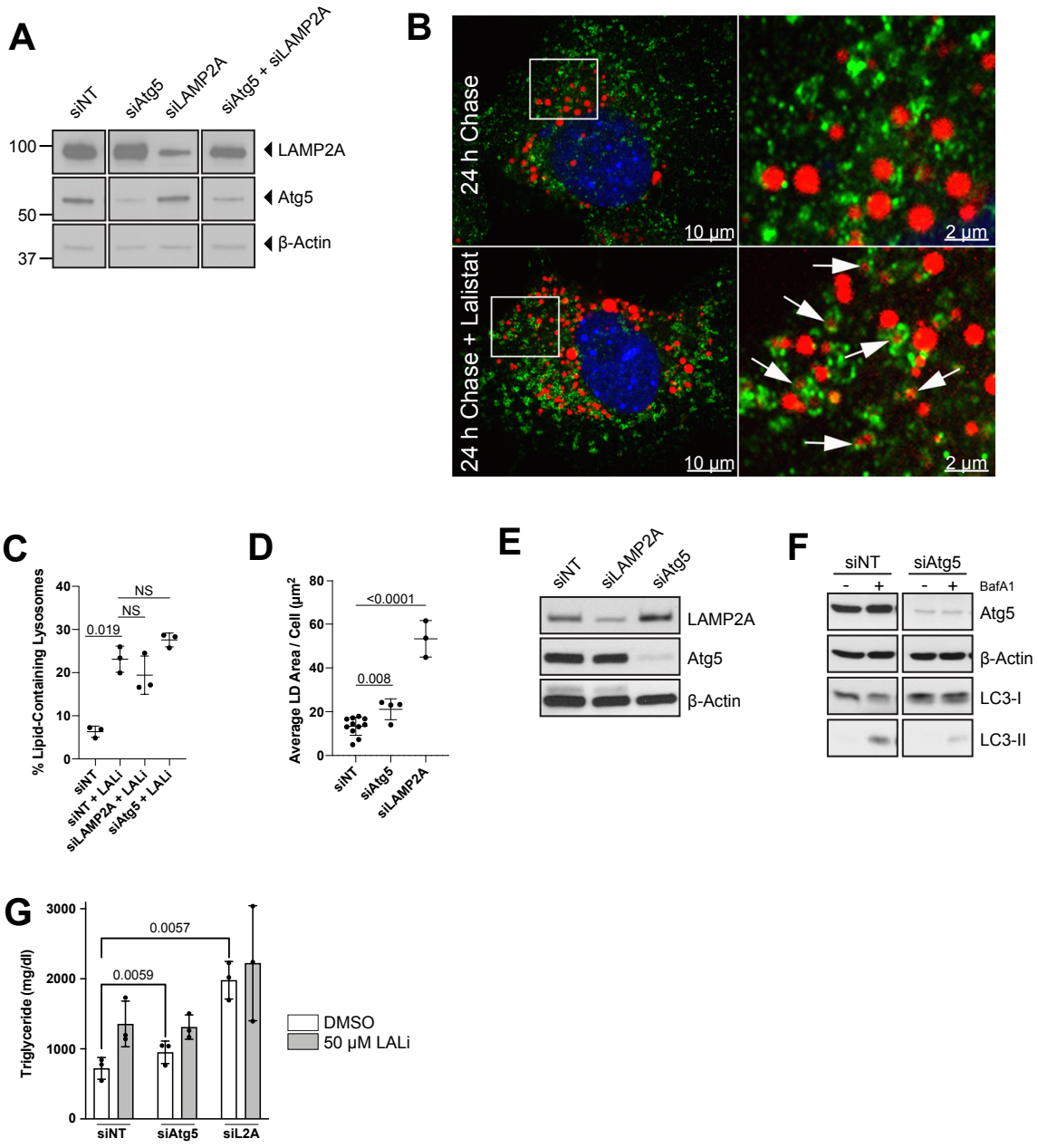

Fig. S4. Knockdown of macroautophagy/CMA machinery does not affect lipid transfer between lysosomes and LDs. (A) Immunoblotting showing the knockdown efficiency of siAtg5, siLAMP2A, or combined knockdown treatments used in Fig. 4A-B. (B-F) AML12 mouse hepatocytes were subjected to 72 h treatment with various siRNAs targeting either Atg5 (macroautophagy) or LAMP2A (CMA) pathways. Cells were loaded for 2 h with 150 µM BSA:oleate + 7.5 µM BODIPY-558/568-C_{12} (red) before washing and chasing for 24 h in unlabeled media +/- 50 µM lalistat to inhibit the lysosomal acid lipase and prevent internalized lipids from being rapidly catabolized. (B) Confocal images of fixed cells showing an accumulation of BODIPY-558/568-C_{12} signal (red) within the lysosomal compartment (antibody staining to LAMP1, green) upon lalistat treatment. Nuclei are stained with DAPI (blue). (C) In the presence of lalistat (LALi), no significant difference in the average percentage of lysosomes containing internalized BODIPY-558/568-C_{12} signal was observed between siNT-treated cells versus those treated with siRNA targeting Atg5 or LAMP2A

(D). (E) Immunoblotting to show the effectiveness of siRNA knockdowns in (B-D) (F) Immunoblotting to verify that Atg5 knockdown impairs LC3 processing. (G) Biochemical measurements of cellular triglyceride content in WT or Atg5- or LAMP2A-depleted cells, both in the presence or absence of lalistat. Displayed statistics from $n = 3$ independent experiments using paired *t*-test. Error bars reflect SD.

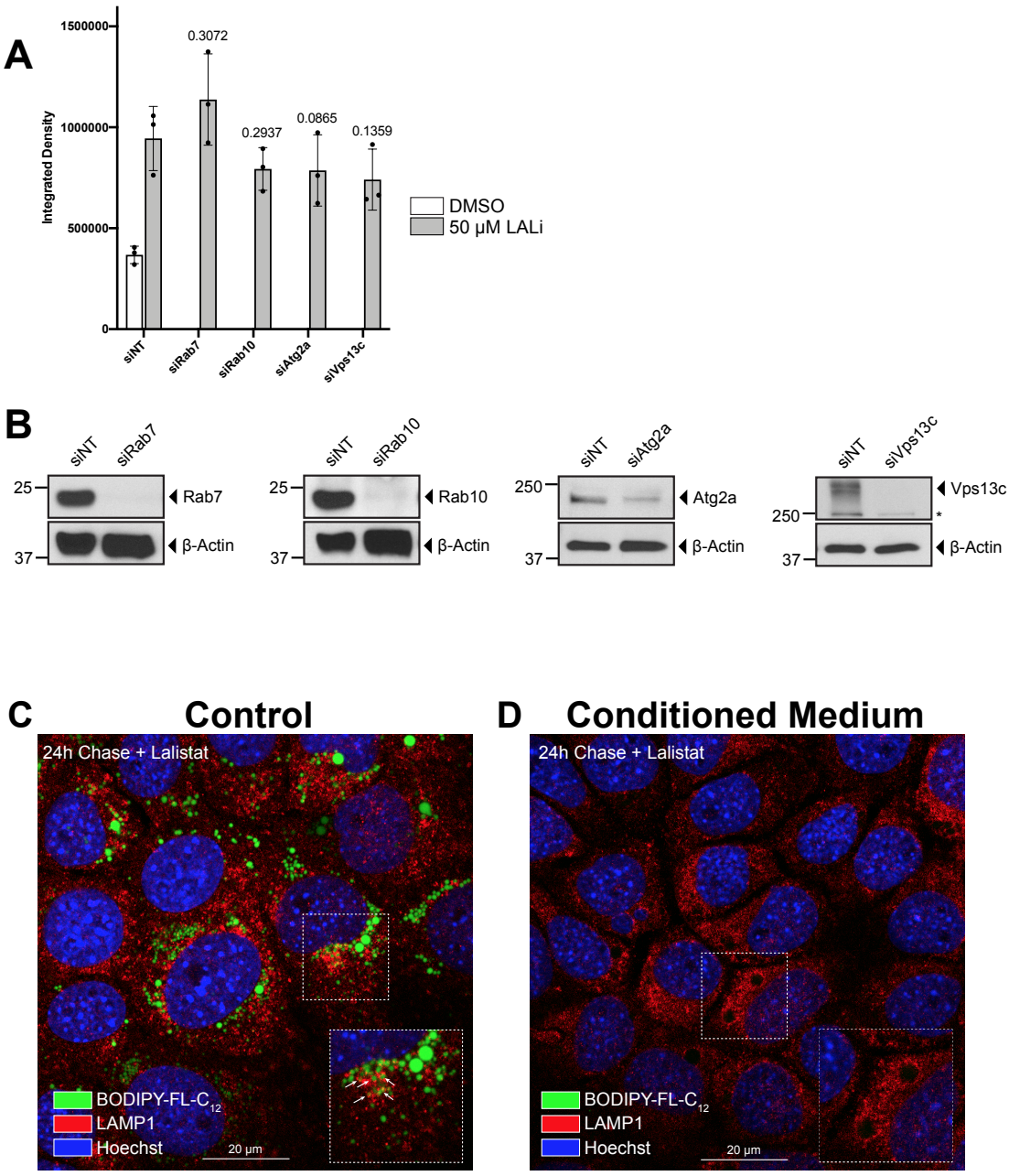

Fig. S5. Knockdown of macrolipophagy and lipid transport machinery does not affect lipid transfer between lysosomes and LDs. (A) Lysosomal lipid uptake upon knockdown of known macrolipophagy (Rab7, Rab10) or lipid transport (Atg2a, Vps13c) factors. Displayed statistics from $n = 3$ independent experiments using paired *t*-test. Error bars reflect SD. (B) Immunoblotting showing the knockdown efficiency of siRab7, siRab10, siAtg2a, or siVps13c treatments. (C-D) Confocal micrographs of AML12 cells loaded with OA, but no BODIPY-FL-C_{12}, then treated with lalistat for 24 h in conditioned medium from cells loaded with both OA + BODIPY-FL-C_{12}. Note the relative absence of green BODIPY-C_{12} from LAMP1-positive vesicles in cells treated with

conditioned medium, suggesting a minimal contribution of lipid or lipoprotein re-uptake in this assay. Representative images are from n=2 independent experiments.

Movie S1 (separate file). Corresponds to still frames from the panel in Figure 1A. Live-cell confocal imaging of 8 μm x 8 μm region of a single AML12 mouse hepatocyte cultured under basal growth conditions and treated with BODIPY-FL-C_{12} and LysoTracker Deep Red to label LDs and lysosomes in the green and magenta channels, respectively. Movie represents 8 min 18 sec of elapsed time with frames captured every 2 sec. Playback is at 20 frames/sec.

Movie S2 (separate file). Corresponds to still frames from the panel in Figure 1H. Live-cell confocal imaging of 6 μm x 6 μm region of a single AML12 mouse hepatocyte transiently expressing the PLIN2-mRFP1-EGFP reporter showing direct contact of a lysosome (blue) with the surface of an LD and subsequent release, 'peeling' away a structure that is RFP^+. Movie represents 28 min 13 sec of elapsed time with frames captured every 13 sec. Playback is at 20 frames/sec.

Movie S3 (separate file). Corresponds to still frames from the panel in Figure 2A. Live-cell confocal imaging of 4 μm x 4 μm region of a single AML12 mouse hepatocyte cultured under basal growth conditions and treated with BODIPY-558/568-C_{12} and LysoTracker Deep Red to label LDs and lysosomes in the green and magenta channels, respectively. Movie represents 24 min 15 sec of elapsed time with frames captured every 5 sec. Playback is at 20 frames/sec.

Movie S4 (separate file). Corresponds to still frames from the panel in Figure 3B. Live-cell confocal imaging of 7 μm x 7 μm region of a single primary rat hepatocyte cultured under basal growth conditions and treated with BODIPY-FL-C_{12} and TMR-Dextran to label LDs and lysosomes in the green and magenta channels, respectively. Movie represents 33 min 20 sec of elapsed time with frames captured every 20 sec. Playback is at 20 frames/sec.